

Driven transport on a flexible polymer with particle recycling: a model inspired by transcription and translation

Lucas D. Fernandes

Departamento de Entomologia e Acarologia, Escola Superior de Agricultura Luiz de Queiroz - Universidade de São Paulo (USP), 13418-900, Piracicaba/SP, Brazil

Luca Ciandrini*

*L2C, Université de Montpellier and CNRS, Montpellier, France and
DIMNP, Université de Montpellier and CNRS, Montpellier, France*

(Dated: 21 March 2018)

Many theoretical works have attempted to coarse grain gene expression at the level of transcription and translation via frameworks based on exclusion processes. Usually in these models the three-dimensional conformation of the substrates (DNA and mRNA) is neglected, and particles move on a static unidimensional lattice in contact to an infinite reservoir. In this work we generalise the paradigmatic exclusion process and study the transport of particles along a unidimensional polymer-like flexible lattice immersed in a three-dimensional particle reservoir. We study the recycling of particles in the reservoir, how the transport is influenced by the conformation of the lattice and, in turn, how particle density dictates the structure of the polymer.

PACS numbers: 05.60.-k, 87.10.-e, 87.16.A-

Introduction. Since their first formulation at the end of the 60's [1], driven lattice models drew the attention of the scientific community for both their relevance in non-equilibrium statistical mechanics, the novelty of their theoretical approaches, and their powerful applications in transport processes [2].

Historically, the prototypical model of unidimensional traffic, the totally asymmetric simple exclusion process (TASEP), has been developed and then extended to describe the collective movement of biological “active particles” such as ribosomes, RNA polymerases or motor proteins, on their respective unidimensional substrates (mRNA, DNA, microtubules or actin filaments). Most of state-of-the-art models describing the gene expression stages of transcription and translation exploit implicitly or explicitly this class of models [3–6]; despite their coarse-grained nature, these frameworks are able to capture the main features of the biological processes.

Although it is incontestable that strands of mRNA or DNA molecules are dynamical objects with complex three-dimensional conformations, common models approximate those tracks with unidimensional unstructured lattices and neglect their polymer-like nature. The interdependence between the lattice conformation and the transport process, however, should be considered when focusing on quantitative modelling aimed to compare experimental data and extract information on the molecular mechanisms. For instance, spatial clustering of genes in transcription factories [7] suggests an interplay between structural conformation of the DNA, gene expression and local recycling of polymerases. Similar effects, including the importance of local ribosome concentrations, can also be expected in translation since the ribosomes are not uniformly distributed in the cy-

toplasm [8]. Furthermore, different conformations assumed by the transcript can explain the gene length-dependence of mRNA translation, as we have recently addressed [9]. Although there are a few models considering the effects of the transport on the substrate dynamics [10] or on local structures [11], its impact on the overall three-dimensional conformation of the lattice has not been explored.

In this work we propose a non-equilibrium model of transport on a polymer-like substrate, which is immersed in a three-dimensional reservoir of diffusing particles. In our derivation we implicitly consider that the timescales of transport and polymer dynamics are well separated: polymerases or ribosomes move at a speed of 10 nm/s, while the dynamics of structural elements of nucleotide chains is orders of magnitude faster [12]. Hence, it is reasonable to assume that the polymer can equilibrate after each particle step, and the local polymer conformation does not affect the motion of particles.

We investigate (i) how the three-dimensional structure of the lattice affects the particle recruitment and the transport process, as well as (ii) how the driven lattice gas impacts, via the particle density, global features of the polymer. We start with a short review of the well known TASEP results, then we couple the system to a three-dimensional diffusive reservoir of particles, and eventually study the interplay between the local concentration of particles, the lattice conformation and the transport process.

Reminder of TASEP results. In its simplest formulation the TASEP consists of a discrete lattice of L sites where particles are injected from one end with rate α , move from one site to the following one -if empty-

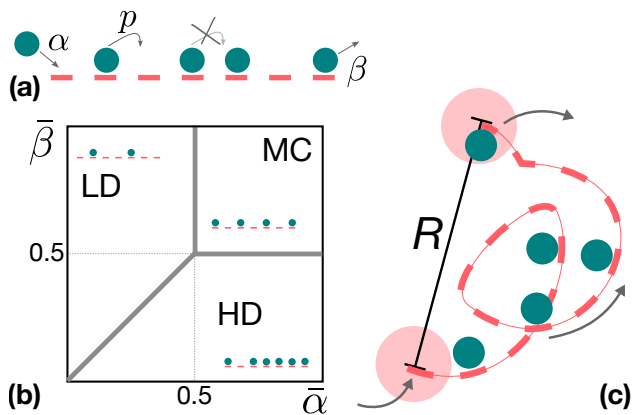


FIG. 1. Scheme of the standard exclusion process (a) and its phase diagram (b), where we emphasised in each phase a typical configuration of the lattice. The same process on a polymer, studied in this paper, is shown in panel (c). R is the end-to-end distance and the red discs represent the reaction volume of the entrance and exit sites (first and last site). The dashed arrow points in the direction of the particle flow, the others highlight particles entering and leaving the first and exit sites.

with rate p , and are eventually removed from the last site with rate β , as illustrated in Fig. 1(a). The system is usually studied by varying the dimensionless parameters $\bar{\alpha} \equiv \alpha/p$ and $\bar{\beta} \equiv \beta/p$, and the phase diagram of the system is known exactly [13]. This is a rich model showing three different regimes (LD, low density; HD, high density; MC, maximal current), as well as first and second order phase transitions. The phase diagram is sketched in Fig. 1(b), and each phase is characterised by a density of particles ρ (average number of particles per site) and current J (particles passing through a site per unit time). Mean-field approaches give the steady-state correct results, which we report in Table I, in the thermodynamic $L \rightarrow \infty$ limit.

Phase	Limits	Density	Current
LD	$\bar{\alpha} < \bar{\beta}, \bar{\alpha} < 1/2$	$\rho = \bar{\alpha}$	$J = p\bar{\alpha}(1 - \bar{\alpha})$
HD	$\bar{\alpha} > \bar{\beta}, \bar{\beta} < 1/2$	$\rho = 1 - \bar{\beta}$	$J = p\bar{\beta}(1 - \bar{\beta})$
MC	$\bar{\alpha}, \bar{\beta} \geq 1/2$	$\rho = 1/2$	$J = p/4$

TABLE I. Summary of the TASEP mean-field results. These relations become exact in the $L \rightarrow \infty$ limit.

Coupling TASEP on a polymer and a diffusive reservoir. In the standard TASEP, the lattice is immersed in an infinite reservoir of particles for which the density determines the entry rate α ; the system can also be coupled to a finite reservoir of particles, and the effects of competition and depletion of a *homogeneous* reservoir without spatial extension has been tackled previously [14]. Here instead we assume that the entry rate depends on the *local* concentration of particles c in a reaction volume V_a

of radius a around the first site, see Fig. 1(c):

$$\bar{\alpha} = \frac{\alpha_0}{p} \frac{1}{V_a} \int_{V_a} c(\mathbf{r}) d^3\mathbf{r}, \quad (1)$$

where $c(\mathbf{r})$ is the concentration of particles in the reservoir at the position \mathbf{r} , and α_0 plays the role of the reaction rate constant. As a lattice, we consider a worm-like chain polymer with persistence length l_p ; the relation between its length L and the end-to-end distance R is given by [15]

$$R = \left[2l_p^2 \left(\frac{L}{l_p} - 1 + e^{-\frac{L}{l_p}} \right) \right]^{\frac{1}{2}} \sim \sqrt{2l_p L}, \quad (2)$$

where we have approximated Eq. (2) since $L \gg l_p$ in many practical cases. For instance, a typical mRNA of length $L = 300$ codons has a persistence length of ~ 1 codon ~ 1 nm [16]. For practical reasons we consider that the origin of the coordinate reference system coincides with the centre of the reaction volume surrounding the entry site.

In order to couple the transport process and the reservoir of particles we need to compute $c(\mathbf{r})$ inside V_a , which can be done by solving the diffusion equation with a sink centred at position $\mathbf{0}$ (S_-) and a source at position \mathbf{R} (S_+):

$$D\nabla^2 c(\mathbf{r}) = S_+(\mathbf{r}) - S_-(\mathbf{r}), \quad (3)$$

where D is the diffusion coefficient of the particles in the reservoir. The sink and the source respectively describe the depletion, where particles are injected in the first site of the lattice, and their appearance around the last site where they abandon the unidimensional track. We exploit the steady-state condition, and considering for the sake of simplicity that the reaction volumes of sink and source are the same, we have $S_{\pm}(\mathbf{r}) := \pm J/V_a$. This connects the diffusion Eq. (3) to the TASEP currents in the three different phases (see Table I), and it shows that the concentration $c(\mathbf{r})$ has different spatial patterns depending on the phase of the transport process. We notice that the source S_+ term in Eq. (3) introduces a spatial feedback, which we also refer to as *particle recycling*, as particles leave the end site and, via diffusion, contribute to the local concentration inside the sink S_- .

The Poisson equation (3) is the same holding in electrostatics to compute the potential $V(\mathbf{r})$ in a system with two spherical and homogeneous distributions of charges [17, 18]. For an individual S_{\pm} , the concentration $c(\mathbf{x})$ at a distance \mathbf{x} from the centre of each sphere can then be written as

$$c(\mathbf{x}) = \begin{cases} \pm \frac{J}{4\pi D|\mathbf{x}|} & \text{outside } S_{\pm} \\ \pm \frac{J}{8\pi D a^3} (3a^2 - x^2) & \text{inside } S_{\pm}. \end{cases} \quad (4)$$

By exploiting the linearity of the diffusion equation and fixing the density far away from the lattice to be c_{∞} ,

we construct the expression of $c(\mathbf{r})$ used to compute the entry rate. Solving the integral in Eq. (1), we obtain the expression for the injection $\bar{\alpha}$ as a function of the current J and the distance R between the entry and exit sites:

$$\bar{\alpha} = \bar{\alpha}_\infty + \frac{J}{p}\Gamma, \quad (5)$$

where $\bar{\alpha}_\infty := \alpha_0 c_\infty / p$ corresponds to the injection parameter usually considered in standard TASEP-based models (i.e. without particle recycling and reservoir depletion), and

$$\Gamma := \begin{cases} \frac{\alpha_0}{4\pi Da} \left(\frac{1}{2d} - \frac{6}{5} \right) & \text{for } d \geq 1 \\ \frac{\alpha_0}{4\pi Da} d^2 \left[\frac{3}{2}d - \frac{1}{5}d^3 - 2 \right] & \text{for } d < 1, \end{cases} \quad (6)$$

where $d := R/2a$ [19]. We recover the standard TASEP when $\Gamma = 0$, or equivalently when we can neglect the spatial inhomogeneities in the reservoir, e.g. for $D \rightarrow \infty$.

Coupling Eq. (5) to the particle current in the LD, HD and MC phases shows how these different regimes affect the spatial feedback and thus the injection $\bar{\alpha}$. Equation (5) will therefore take different forms according to the phase of the TASEP (see Table I):

$$\bar{\alpha} = \begin{cases} \bar{\alpha}_\infty + \bar{\alpha}(1 - \bar{\alpha})\Gamma & \text{(LD)} \\ \bar{\alpha}_\infty + \bar{\beta}(1 - \bar{\beta})\Gamma & \text{(HD)} \\ \bar{\alpha}_\infty + \Gamma/4 & \text{(MC)}. \end{cases} \quad (7)$$

Only in the LD phase we need to solve a second order equation to find $\bar{\alpha}$ and obtain

$$\bar{\alpha}_{LD} = \frac{(\Gamma - 1) \pm \sqrt{(1 - \Gamma)^2 + 4\bar{\alpha}_\infty\Gamma}}{2\Gamma}. \quad (8)$$

We recall that the solution $\bar{\alpha}_{LD}$ is relevant only if $\bar{\alpha} < \bar{\beta}$ and $\bar{\alpha} < 1/2$ (otherwise the system is in HD or MC); we always find only one physical solution $\bar{\alpha}_{LD}$.

The phase boundaries given in Table I can be rewritten in terms of the new parameters and in Fig. 2 we show the phase diagram of the system in the $\{\bar{\alpha}_\infty, \bar{\beta}\}$ plane for different values of Γ . As expected from Eq. (5), if $\Gamma = 0$ we recover the phase diagram of the TASEP (black lines) with $\bar{\alpha}_\infty$ playing the role of the entry rate of the standard TASEP. This situation is also met when the reaction volumes of the entrance and exit sites match, i.e. for a fully circularised lattice suppressing the depletion of the reservoir [20]. The dimensionless parameter Γ is otherwise always negative, and it weights the interplay between particle recycling and depletion around the entrance site of the lattice, which is proportional to J . When $\Gamma < 0$ the LD-HD transition lines are convex and the MC regime is reached for increasingly larger values of $\bar{\alpha}_\infty$.

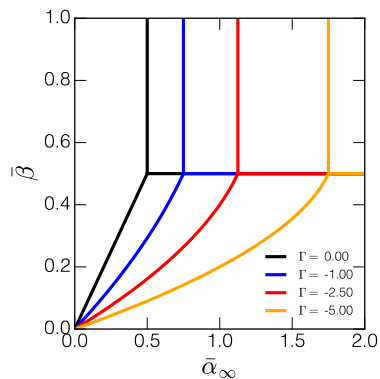


FIG. 2. Phase diagram of the TASEP with feedback in the $\{\bar{\alpha}_\infty, \bar{\beta}\}$ plane for different values of Γ (color online).

Coupling polymer conformation and transport. In the previous sections we assumed that the transport process does not interact with the lattice conformation. Here we imagine that the particle density stiffens the polymer and hence controls the global configuration of the lattice. In turn this will have a repercussion on the particle recycling that depends on R . We do not consider local secondary structures of the lattice, assuming that the particles can efficiently unfold them or that folding competes with the particle flow [11] (as in the case of ribosomes moving on the mRNA).

If the persistence length of the lattice l_p is larger than the particle's footprint ℓ , then the transport process does not affect the end-to-end distance: the particles' positions do not impact the three-dimensional conformation of the polymer and the recruitment of particles depends, as described in Eq. (5), on R given by Eq. (2). Instead, if $\ell > l_p$, the presence of a particle on the lattice flattens the region of the lattice corresponding to its footprint; as a consequence, the particle density ρ influences the end-to-end distance, changing the features of particle recycling. We define an effective persistence length l_{eff} by considering the portion of the lattice occupied by particles ($\rho\ell$), which has a persistence length equal to the particle length ℓ , and the portion of the lattice that is empty $(1 - \rho\ell)$, with a persistence length l_p :

$$l_{\text{eff}} := \rho\ell^2 + (1 - \rho\ell)l_p.$$

This equation is valid only when $\ell \geq l_p$, and otherwise $l_{\text{eff}} = l_p$. We can then redefine

$$R := \sqrt{2l_{\text{eff}}L} = R_0 F_\rho, \quad (9)$$

where

$$R_0 := \sqrt{2l_p L} \quad (10)$$

$$F_\rho := \left[1 + \rho\ell \left(\frac{\ell}{l_p} - 1 \right) \right]^{\frac{1}{2}}. \quad (11)$$

Here R_0 is the mean end-to-end distance of an empty polymer and $F_\rho = R/R_0 \geq 1$ is a measure of how much

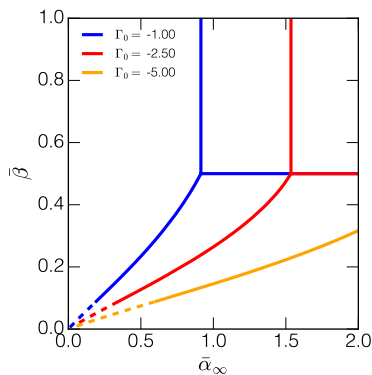


FIG. 3. Phase diagram of the TASEP on a flexible polymer in the $\{\bar{\alpha}_\infty, \bar{\beta}\}$ plane for different values of Γ_0 (color online) and by fixing $a = 1.5$, $\ell = 1$, $l_p = 0.1$ and $L = 25$ (giving $R_0 \simeq 2.24$). All lengths are expressed in terms of lattice sites. We use a dashed line when the system is in the $d < 1$ case, and a full line otherwise.

the polymer is flattened by the particle occupancy. In this work we use either R or F_ρ as proxies for the polymer conformation. The parameter Γ then reads

$$\Gamma = \begin{cases} \Gamma_0 + \frac{\alpha_0}{4\pi D} \frac{1}{R_0} \left(\frac{1 - F_\rho}{F_\rho} \right) & d \geq 1 \\ \left[\Gamma_0 + \frac{\alpha_0 d_0^3}{4\pi D a} \left[\frac{3}{2}(F_\rho - 1) - \frac{1}{5} d_0^2 (F_\rho^3 - 1) \right] \right] F_\rho^2 & d < 1, \end{cases} \quad (12)$$

where Γ_0 is obtained by calculating the parameter Γ from Eqs. (6) by setting $R = R_0$ and $d_0 := R_0/2a$. We emphasise that we recover the results of the previous section when $\ell \leq l_p$ and therefore the transport process and polymer properties are decoupled. We can still use Eqs.(7) to compute the entry parameter in the different phases, although, this time, Γ is a function of ρ , which also depends on the phase as given in Table I. For instance, to find the value of $\bar{\alpha}$ in LD, now we need to solve $\bar{\alpha} = \bar{\alpha}_\infty + \bar{\alpha}(1 - \bar{\alpha})\Gamma$ with Γ from Eq. (12) computed with $\rho = \bar{\alpha}$. By solving those equations it is possible to determine the phase boundaries of the three TASEP phases, now considering the feedback that the polymer conformation dictates on the exclusion process. We show this phase diagram in Fig. 3 for different values of Γ_0 and for parameters that could represent ribosome translating an mRNA (if one rescales the length of the mRNA by the size of a ribosome and considers a typical interaction length a of the order of the ribosome size).

This phase diagram is qualitatively similar to the one obtained without coupling the polymer conformation and the exclusion process shown in Fig. 2. However, there are relevant quantitative changes between the two processes. We remark that the TASEP-limit is achieved when the diffusion coefficient D tends to infinity, which would lead Γ to zero, resulting in a negligible feedback term.

Polymer conformation as a proxy for transport regimes. If, on one hand, the exclusion process is affected by the polymer conformation via the spatial feedback depending on R , on the other hand the density of particles ρ impacts the typical polymer conformation as given in Eq. (9). As shown in Fig. 4(a), obtained by numerically solving Eq.(11), with increasing $\bar{\alpha}_\infty$ we observe that the polymer conformation undergoes a transition from a compact to a more flattened shape ($F_\rho > 1$) driven by the accumulation of particles on it. This transition can be abrupt when the transport process crosses the LD-HD transition line (fuchsia line). We emphasise that $\bar{\alpha}_\infty$ is proportional to the particle concentration, meaning that features of the polymer conformation will vary by changing the particle concentration c_∞ or in general the entry rate α .

In Fig. 4(b) we show how regimes of the polymer conformation coincide to the different phases of the exclusion process. When the lattice is empty ($\bar{\alpha}_\infty = 0$) or its persistence length is larger than the particles' size, then $F_\rho = 1$ and the lattice follows standard polymer physics. Otherwise, the polymer is coupled to the transport process via its particle density, and the end-to-end distance changes by a factor F_ρ . In other words, particles flatten the lattice around their positions, inducing a change in the polymer conformation; in turn this has an influence on the feedback controlled by the end-to-end distance R presented in the previous sections.

From Fig. 4 we can appreciate that R follows the different dynamical TASEP phases: when the system is in LD, the polymer is in its compactest shape, while the ends get separated in the MC and the polymer becomes more and more stretched deep in the HD phase, as sketched in Fig. 4(b).

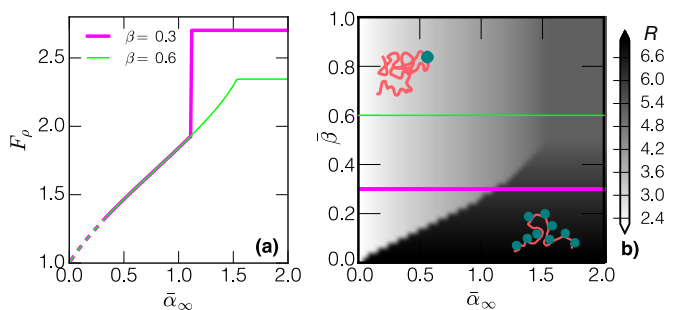


FIG. 4. Transport effects on polymer conformation (colour online). The factor F_ρ as a function of $\bar{\alpha}_\infty$ (a) shows an abrupt transition when the TASEP LD-HD transition occurs (fuchsia line). The dashed curves represent the $d < 1$ case. In panel (b) we show in a colour map how the end-to-end distance R changes in the $\{\bar{\alpha}_\infty, \bar{\beta}\}$ plane. The horizontal lines correspond to $\beta = 0.3, 0.6$ respectively, for which F_ρ is shown in panel (a) maintaining the same colour code. In both panels $\Gamma_0 = -2.5$ and the other parameters correspond to the ones used in Fig. 3. In the upper left and bottom right corners of panel (b) we sketch a cartoon of the polymer configurations (in red) with particles on it (green) corresponding to those regions of the diagram. R is given in lattice-site units.

Discussion. We have developed a novel approach to study the interdependence between transport on a uni-dimensional substrate (the exclusion process) and the three-dimensional conformation of the lattice on which the particles move. When coupling the exclusion process to a reservoir of diffusive particles we find a depletion of their local concentration around the entry site, which affects the recruitment of particles in the lattice. We then propose a coupling between driven transport and polymer that influences the three-dimensional conformation of the polymer. This in turn acts on the strength of the spatial feedback.

Our framework considers both local depletion of particles and substrate conformation; such an interplay with the transport process has not been investigated previously. In our approach, the substrate thus acquires a key role. We show that, in this perspective, physical properties of the lattice such as its length or persistence length cannot be overlooked –as usually done in coarse grained modelling– to provide a complete description of the transport process. Following our approach the conformational state of the polymeric lattice becomes informative of the properties of the transport occurring on it. Thus, the lattice conformation could be exploited to estimate regimes of transport. For instance, there is evidence that typical structures of polysomes (mRNAs with active ribosome translating) depend on the transport process and in particular on the ribosome recruitment [21] (this effect can be experimentally achieved by antibiotics, which effectively decrease the amount of ribosomes c_∞ [22]).

Moreover, the role of mRNA circularisation or transcription factories in determining gene expression is still largely unknown. The full circularisation of eukaryotic transcripts is assisted by molecular partners promoting the interaction between their ends; when this interaction is disrupted the translation efficiency strongly decreases. This is consistent with our theory, which predicts optimal ribosome recycling with full circularisation ($\Gamma = 0$). However, this effect competes with the increase of the polymer effective persistence length induced by high density translation, that reinforces the importance of considering the process on a flexible substrate. A prototypical model of circularisation has been studied in [9]. A similar situation might be encountered in DNA transcription, where the local concentration of polymerases and their recycling seem to be relevant in determining transcription factories.

Future works might provide new insights by exploring the extension of the model to inhomogeneous TASEP [23], TASEP with extended particles [24] and finite resources [14].

Acknowledgements. LDF acknowledges the funding provided by the São Paulo Research Foundation (FAPESP - grant 2015/26989-4) and LC the CNRS for having

granted him a “demi-délégation”. The authors thank Philip Greulich and Norbert Kern for their useful comments on the manuscript.

* luca.ciandrini@umontpellier.fr

- [1] C. T. MacDonald, J. H. Gibbs, and A. C. Pipkin, *Biopolymers* **6**, 1 (1968); C. T. MacDonald and J. H. Gibbs, *Biopolymers* **7**, 707 (1969).
- [2] T. Chou, K. Mallick, and R. K. P. Zia, *Rep. Prog. Phys.* **74**, 116601 (2011).
- [3] N. Mitarai, K. Sneppen, and S. Pedersen, *J. Mol. Bio.* **382**, 236 (2008).
- [4] S. Reuveni, I. Meilijson, M. Kupiec, E. Ruppin, and T. Tuller, *PLoS Comput. Biol.* **7**, e1002127 (2011).
- [5] C. Leduc, K. Padberg-Gehle, V. Varga, D. Helbing, S. Diez, and J. Howard, *Proc. Nat. Acad. Sci. USA* **109**, 6100 (2012).
- [6] L. Ciandrini, I. Stansfield, and M. C. Romano, *PLoS Comput. Biol.* **9** (2013).
- [7] H. Sutherland and W. A. Bickmore, *Nature Rev. Genet.* **10**, 457 (2009).
- [8] S. Bakshi, A. Siryaporn, M. Goulian, and J. C. Weisshaar, *Mol. Microbiol.* **85**, 21 (2012).
- [9] L. D. Fernandes, A. P. S. d. Moura, and L. Ciandrini, *Sci. Rep.* **7**, 17409 (2017).
- [10] A. Melbinger, L. Reese, and E. Frey, *Phys. Rev. Lett.* **108**, 258104 (2012).
- [11] G. Von Heijne, L. Nilsson, and C. Blomberg, *J. Theor. Biol.* **68**, 321 (1977); F. Turci, A. Parmeggiani, E. Pitard, M. C. Romano, and L. Ciandrini, *Phys. Rev. E* **87** (2013).
- [12] H. M. Al-Hashimi and N. G. Walter, *Curr. Opin. Struct. Biol.* **18**, 321 (2008).
- [13] R. A. Blythe and M. R. Evans, *J. Phys. A* **40**, R333 (2007).
- [14] P. Greulich, L. Ciandrini, R. J. Allen, and M. C. Romano, *Phys. Rev. E* **85** (2012).
- [15] M. Rubinstein and R. H. Colby, *Polymer Physics* (Oxford University Press, New York, 2003).
- [16] F. Vanzi, Y. Takagi, H. Shuman, B. S. Cooperman, and Y. E. Goldman, *Biophys. J.* (2005).
- [17] J. D. Jackson, *Classical Electrodynamics* (Wiley, New York, 1962).
- [18] T. J. Eisler, *An Introduction to Green's Functions* (Institute of Ocean Science and Engineering, The Catholic University of America, 1969).
- [19] See Supplementary Material for a derivation of Eqs. (6).
- [20] L. D. Fernandes and L. Ciandrini, in preparation (2018).
- [21] G. Viero, L. Lunelli, A. Passerini, P. Bianchini, R. J. Gilbert, P. Bernabò, T. Tebaldi, A. Diaspro, C. Pedersoli, and A. Quattrone, *J. Cell Biol.* **208**, 581 (2015).
- [22] P. Greulich, M. Scott, M. R. Evans, and R. J. Allen, *Mol Syst Biol* **11** (2015), 10.15252/msb.20145949.
- [23] J. Szavits-Nossan, L. Ciandrini, and M. C. Romano, *Phys. Rev. Lett.* **120**, 128101 (2018); J. Szavits-Nossan, M. C. Romano, and L. Ciandrini, arXiv:1803.00887 (2018).
- [24] L. B. Shaw, R. K. Zia, and K. H. Lee, *Phys. Rev. E* (2003); D. D. Erdmann-Pham, K. D. Duc, and Y. S. Song, arXiv:1803.05609 (2018).